PROCEEDINGS OF SCIENCE

Towards a high-precision description of the ρ and K^* resonances

Nelson Pitanga Lachini,[a,b,*] **Peter Boyle,**[a,c] **Felix Erben,**[a,d] **Vera Gülpers,**[a] **Maxwell T. Hansen,**[a] **Fabian Joswig,**[a] **Michael Marshall**[a] **and Antonin Portelli**[a,d,e]

[a] *School of Physics and Astronomy, University of Edinburgh, Edinburgh EH9 3JZ, UK*

[b] *DAMTP, University of Cambridge, Centre for Mathematical Sciences, Wilberforce Road, Cambridge, CB3 0WA, UK*

[c] *Brookhaven National Laboratory, Upton, NY 11973, USA*

[d] *CERN, Theoretical Physics Department, Geneva, Switzerland*

[e] *RIKEN Center for Computational Science, Kobe 650-0047, Japan*

E-mail: np612@cam.ac.uk

We summarise our determination of the ρ and K^* resonance parameters from lattice QCD at a physical pion mass. The methods for computing correlation functions and extracting energy levels from an RBC-UKQCD domain-wall fermion ensemble are reviewed. We use the finite-volume spectra from lattice irreducible representations with only leading P-wave contributions to constrain the elastic $K\pi$ and $\pi\pi$ scattering amplitudes and the associated resonance pole positions. Lastly, our estimation of systematic errors through a model-averaging technique is outlined and a conclusion is given.

European network for Particle physics, Lattice field theory and Extreme computing (EuroPLEx2023)
11-15 September 2023
Berlin, Germany

*Speaker

PoS(EuroPLEx2023)017

1. Introduction

Hadronic resonances are unstable particles that decay through the strong force, manifesting the "physics of binding and decay" [1] from QCD. Most observed hadrons are resonances and they are expected to produce typical enhancements on experimental cross-sections in which they act as intermediate states [2]. For example, the $\rho(770)$ resonance is present in electron-positron scattering and plays a role in the calculation of the muon $g-2$ [3]. Both $\rho(770)$ and $K^*(892)$ resonances feature in processes such as B-meson decays, which are being examined for potential signs of physics beyond the Standard Model [4]. In a process-independent way, resonances can be associated to singularities of analytically continued scattering amplitudes. In principle, this does not depend on a specific realisation or modelling of the scattering process, and thus provides a more universal description of resonances.

Lattice quantum chromodynamics (QCD) allows for first-principle QCD calculations achieved through a systematically improvable method. It consists of discretising a finite spacetime in Euclidean signature, which can be translated into a numerical problem. However, the study of dynamical properties is considerably challenged by the Euclidean metric. The understanding of finite-volume effects on the lattice spectrum [5–10] allied to the creation of novel algorithms in lattice QCD [11, 12] have allowed for rigorous theoretical determinations of resonances in the past decade [1, 13], including the ρ and K^* [14–17]. However, the physical limits of scattering determinations from the lattice are still largely unexplored due to their high computational cost. In particular, most works to date have employed higher-than-physical pion masses. Due to the non-trivial quark-mass dependence of resonance poles from QCD dynamics, extrapolations from large masses can introduce non-negligible systematics. Performing lattice computations at physical pion masses is thus a fundamental step towards reliable Standard Model predictions that depend on resonance features.

In this proceedings, we review the basic aspects of our determination of the $\rho(770)$ and $K^*(892)$ resonance parameters using lattice QCD at a physical pion mass [I]. This is performed on the physical-point RBC-UKQCD domain-wall fermion lattice detailed in Table 1. After an initial numerical exploration involving the development of dedicated software [20, 21], we built a diversified operator basis and computed two-point correlation functions in various momentum frames using the distillation method [11]. The low-lying lattice spectrum was extracted by solving a generalised eigenvalue problem (GEVP) on the associated matrix of correlators. Finally, the so-called Lüscher formalism was employed to constrain the $\pi\pi, I=1$ and $K\pi, I=1/2$ phase shifts in P-wave, where the ρ and K^* feature as resonances, respectively. The analytical continuation of different phase-shift models leads to the resonance pole positions, which are taken as our final result. We outline the model-averaging procedure that results in the estimation of analysis systematics involved on this lattice calculation.

$N^3 \times N_t$	a	L	$m_\pi L$	am_π	am_K
$48^3 \times 96$	≈ 0.114 fm	5.476(2) fm	3.863(5)	138.5(2) MeV	498.9(4) MeV

Table 1: Physical-point domain wall $N_f = 2+1$ ensemble used in this work [22].

[I] Now published in Refs. [18, 19].

2. Lattice Spectroscopy

2.1 Interpolators

We start by considering a basis of operators with significant overlap to the low-lying states with the same quantum numbers as the ρ and K^*. We use local operators of the type

$$O_V(x) \sim \bar{q}_V(x)\boldsymbol{\gamma} q'_V(x), \quad V \in \{\rho^+, K^{*+}\}, \tag{1}$$

where q is a light or strange quark field and $\boldsymbol{\gamma} = (\gamma_x, \gamma_y, \gamma_z)$ are the spatial Dirac matrices. Additionally, we employ two-bilinear interpolators

$$O_{MM'}(x, y) \sim \bar{q}_1(x)\gamma_5 q_2(x)\ \bar{q}'_1(y)\gamma_5 q'_2(y), \quad MM' \in \{\pi\pi, K\pi\}, \tag{2}$$

which contain an appropriate linear combination of pseudoscalar bilinears interpolating states with the K and π quantum numbers. Operators with well-defined spatial momentum are obtained by Fourier-projections of the various spatial coordinates. Note that the isospin projection into $I = 1/2$ for $K\pi$ and $I = 1$ for $\pi\pi$ is left implicit in the above. The operator labels are based on a conventional quark-model picture of the hadronic states, and cannot be directly related to lattice QCD states. In fact, previous studies showed that at least both bilinear and two-bilinear type of operators are necessary to reliably extract the low-lying lattice spectrum [23].

Channel	Irreps $\Lambda[\mathbf{d}]$
$K\pi$	$T_{1u}[000]$, $E[001]$, $B_1[110]$, $B_2[110]$, $E[111]$, $E[002]$
$\pi\pi$	all above + $A_1[001]$, $A_1[110]$, $A_1[111]$, $A_1[002]$

Table 2: Irreps of the cubic symmetries (times spatial inversion) considered in this work [24]. They do not feature mixed even and odd infinite-volume partial waves, and thus only contain leading P-wave contributions [25].

The formulation of QCD on a finite volume breaks rotational symmetry, restricting the allowed momenta carried by lattice states. For integer intrinsical spin, states at rest will be labeled by irreducible representations (irreps) Λ of the cubic group, instead of irreps of $SO(3)$ identified by the angular momentum J [26]. A similar consideration can be done for moving states now in relation to subgroups of the cubic symmetry together with spatial inversions [27]. The interpolators defined in Eqs. (1) and (2) do not transform irreducibly under these symmetries and thus need to be projected into definite Λ. Given that each bilinear in those interpolators can be momentum-projected into different spatial $\mathbf{p}$, the irrep projection can be achieved through the group-theoretic formula [24]

$$O^\Lambda(\mathbf{p}_1, \mathbf{p}_2, \ldots, t) = \sum_{R \in G} B^\Lambda(R)\, \hat{R} O(\mathbf{p}_1, \mathbf{p}_2, \ldots, t) \hat{R}^{-1}, \tag{3}$$

where R represents elements of the cubic (sub) group G and the coefficients B^Λ encode the associated Clebsch-Gordan coefficients. This yields $O^\Lambda_V(\mathbf{P})$ and $O^\Lambda_{MM'}(\mathbf{p}_1, \mathbf{p}_2, t)$, where the total momentum is given by $\mathbf{P} = \mathbf{p}_1 + \mathbf{p}_2$. We only consider irreps whose mapping into infinite-volume angular momentum is dominated by P-wave, and where $\mathbf{P}^2 \leq 4(2\pi/L)^2$, as listed in Table 2.

2.2 Distillation

It is a challenging task to compute two-point correlation functions $\langle O'(t')O^\dagger(t)\rangle$ with the operators defined above, particularly when $O' = O = O_{MM'}$. Partly, this is due to the need of estimating quark propagators $D^{-1}(x,x') = \langle q(x)\bar{q}(x')\rangle$ from all lattice sites x' to all lattice sites x. We use the so-called distillation method [11, 28], defined by the smearing kernel onto the low-mode subspace of the gauge-covariant $3D$-Laplacian $-\boldsymbol{\nabla}^2_{ab}(t)$,

$$\Box(t) = \sum_{k=1}^{N_{\text{vec}}} v_k(t)v_k(t)^\dagger\,, \tag{4}$$

where $v_k(t)$ are the N_{vec} low-lying eigenvectors of $\boldsymbol{\nabla}^2_{ab}$. Together with link smearing [29], this helps suppressing high-lying modes and thus enhances the information from the low-energy states contained in the correlation functions.

In distillation, the quark propagator is numerically computed through inversions of the Dirac operator D over the Laplacian eigenvectors, *i.e.* $D^{-1}v_k$. This leads to the so-called *perambulator*

$$\tau^{[d_t]}_{(f)}(t) = v(t)^\dagger D^{-1}(t,d_t)v(d_t)\,\delta_{td_t} \tag{5}$$

where the index $[d_t]$ trivially projects out a time slice t [II]. This smeared propagator-like object can be used to assemble "sink" vectors $\varphi^{[d_t]}_{(f)}(t) \sim v(t)\tau^{[d_t]}_{(f)}(t)$, which can be combined with the "source" vectors $\varrho^{[d_t]}(t) \sim v(t)\delta_{td_t}$ to form a *meson field*

$$\left(\mathcal{M}^{(f)}_\Gamma\right)^{[d_t^1][d_t^2]}(\mathbf{p},t) \sim \sum_{\mathbf{x}} e^{-i\mathbf{p}\cdot\mathbf{x}}\,\mathrm{tr}\left[\varrho^{[d_t^1]}(\mathbf{x},t)^\dagger\,\Gamma\,\varphi^{[d_t^2]}_{(f)}(\mathbf{x},t)\right], \tag{6}$$

where the spatial argument $\mathbf{x}$ was pulled out to express the momentum projection into $\mathbf{p}$. This is the building block for computing all correlators in this work, and in Figure 1 an example Wick contraction appearing in a $K\pi$-like correlation function is given.

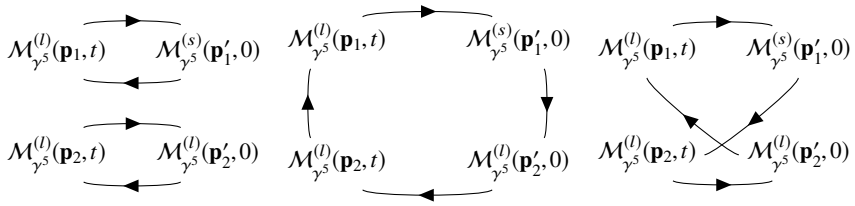

Figure 1: Wick contraction diagram contributing to the $\langle O_{K\pi}(\mathbf{p}_1,\mathbf{p}_2,t)\,O_{K\pi}(\mathbf{p}'_1,\mathbf{p}'_2,0)^\dagger\rangle$ correlator in terms of meson fields (6). A line means matrix product and a closed loop means a trace over all dilution indices. The quark flavour labels $f = l,s$ mean light and strange, respectively.

We developed distillation within the workflow management system `Hadrons` [30–32] on top of the `C++` lattice library `Grid`, which implements domain-wall fermions and various other lattice utilities [33]. In the production phase, we adopted $N_{\text{vec}} = 64$ (see [20, 21]) and processed

[II] The dilution-index notation is used in the stochastic version of distillation [28], and we employ it here only for defining the matrix structure of Eq. (6). From the full dilution index, $[d] = [d_t, d_\alpha, d_k]$, we leave the trivial indices d_α and d_k implicit in the matrix notation.

90 gauge configurations of the physical pion ensemble (see Table 1). All $N_t = 96$ source time translations of the Dirac propagators were computed, allowing for averaged correlators, *i.e.* $N_t^{-1} \sum_{\xi=1}^{N_t} \langle O'(\xi + t) O^\dagger(\xi) \rangle$, and consequently improved statistics.

In Figure 2 we illustrate a schematic `Hadrons` workflow for producing the meson field Eq. (6). Based on the dataflow programming [30], the data gets transformed in the direction of the arrows. It starts with input parameters and modules (orange), which are followed by distillation modules (red), and finally a meson field output is saved to disk on a dedicated file format (violet). The perambulator module either computes the necessary Dirac matrix inversions (via `solver`) or loads a file from disk. The `DistilMesonFieldRelative` module with standard input yields meson fields $M_\Gamma^{[t][t']}(\mathbf{p}, t)$, where quark lines have support only on one sink time slice t' for a given time source t [31].

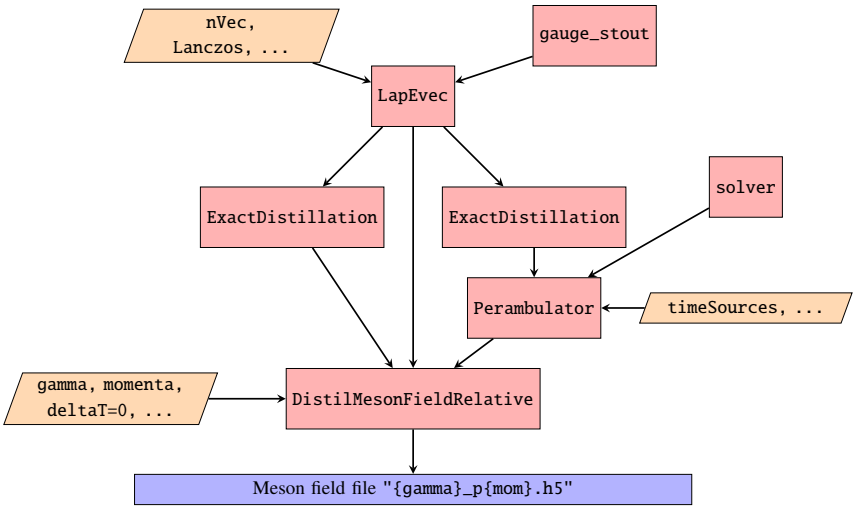

Figure 2: Exact distillation workflow for a meson field production in `Hadrons`, starting from a gauge configuration and distillation-related parameters [31]. For an example of code implementing this workflow, see Ref. [32].

2.3 Generalised Eigenvalue Problem

We assemble the matrix of two-point functions $C_{XZ}(t) \equiv \langle O_X(t) O_Z(0)^\dagger \rangle$ from the correlation functions computed through distillation, where the compound indices X, Z collectively represent spatial momenta projection, flavour bilinear and irrep quantum numbers of operators. We then solve the so-called generalised eigenvalue problem (GEVP)

$$C(t) u^n(t) = \lambda^n(t) C(t_0) u^n(t) \,, \tag{7}$$

where the eigenvalues have the asymptotic form $\lambda^n(t) \to Z_n \exp(-E^n t)$ for $t, t_0 \gg 1$ with corrections exponentially suppressed by nearby energy gaps [34, 35]. In this work, the auxiliary time is fixed to a sufficiently large value $t_0 = 3$ and the asymptotic t-dependence of λ^n is used to statistically constrain the energies E^n. The GEVP is solved separately for each cubic symmetry irrep from Table 2.

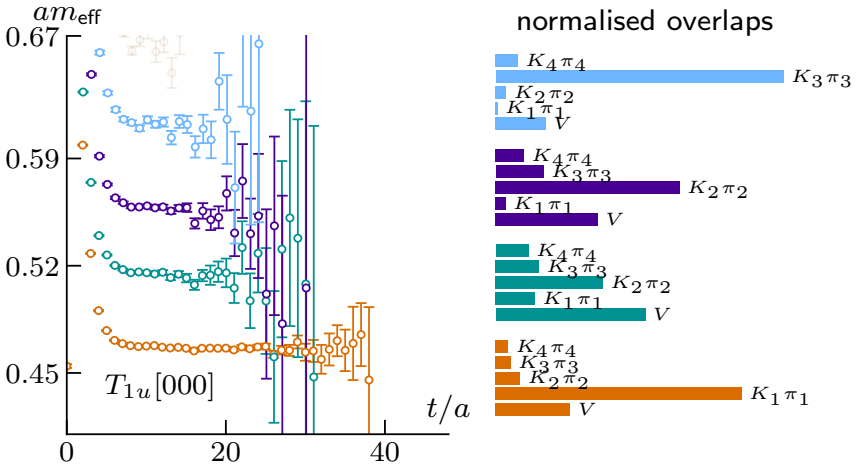

Figure 3: Overlaps from each operator (right) to the states represented by effective masses (left) in the $T_{1u}[000]$ rest-frame irrep with K^* quantum numbers. We omit the error bars on the overlaps as they do not affect the visualisation. The effective energies were boosted to CM in the same way as E^n_{cm}.

To statistically estimate each lattice energy, we fit the single-exponential model $\lambda^n_{\text{fit}}(t) = Z^n_{\text{fit}} e^{-tE^n_{\text{fit}}}$ to each corresponding λ^n within a certain range $[t_{\text{min}}, t_{\text{max}}]$ of time slices ("fit range"). This is implemented through the minimisation of a standard chi-squared function, where correlations between time slices are taken into account through a bootstrap estimate of the covariance matrix [18]. The statistical uncertainties on the data are propagated into E^n_{fit} also via the bootstrap method. For later use, the resulting model energies E^n_{fit} are boosted to the CM via the continuum dispersion relation, defining $E^n_{\text{cm}} = \sqrt{(E^n_{\text{fit}})^2 - \mathbf{P}^2}$, on each lattice irrep.

The onset of the large-t regime can be visualised through the log effective mass

$$m^n_{\text{eff}}(t) = \log \frac{\lambda^n(t)}{\lambda^n(t+1)}, \tag{8}$$

which is exemplified in Figure 3 for the $K\pi$ system. The effective overlap of the state n to the operator O_i can be given by

$$Z^{ni}_{\text{eff}}(t) = [u^\dagger_n(t) C(t_0)]_i \, e^{m^n_{\text{eff}}(t) t_0/2}, \tag{9}$$

whose value at a sufficiently large times is also shown in Figure 3 for a particular irrep. This illustrates the relative importance of a given operator towards extracting the low-lying spectrum.

3. Scattering

The study of scattering processes is central to this work. In scattering theory, it is usual to define in/out states characterised by well-defined spatial momenta. Interactions are taken to have finite duration and, at asymptotic times $t \to \pm\infty$, such states are assumed to be sufficiently far apart [36]. The scattering S-matrix is then defined as the map between in/out states, *i.e.*

$$\langle p_1 p_2 \ldots ; out \,|\, q_1 q_2 \ldots ; in \rangle \equiv \langle p_1 p_2 \ldots \,|\, S \,|\, q_1 q_2 \ldots \rangle \,, \tag{10}$$

related to the so-called *scattering amplitude* t via $S = \mathbb{1} + it$. In phenomenology, one is often interested in the partial-wave components of the quantities above, labeled by ℓ. For elastic $2 \to 2$ scattering, the t-matrix can be written as

$$t_\ell(E_{\text{cm}}) = \frac{1}{\cot \delta_\ell(E_{\text{cm}}) - i}\,, \tag{11}$$

where the phase shift $\delta_\ell(E_{\text{cm}})$ depends only on the CM energy.

3.1 Finite-volume Method

Lattice QCD calculations are done on a finite volume and Euclidean spacetime metric. This yields the extraction of scattering amplitudes from lattice simulations intrinsically challenging. Note that resonances are *not* eigenstates of the Hamiltonian, which antecipates an intricate manifestation of resonance physics in lattice observables.

Because of the Euclidean signature, it is a tough task to effectively translate lattice correlation functions to Minkowski spacetime, where conventional quantum field theory techniques can be used [37, 38]. The compactification of QCD into a finite volume further distorts its spectral properties. For example, in a three-dimensional spatial box of size L with a field obeying periodic boundary conditions, momenta are restricted to the discrete values $\mathbf{p} = \frac{2\pi}{L}\mathbf{n}, \quad \mathbf{n} \in \mathbb{Z}_3$,. Other typical features of Euclidean correlators on the complex plane are also affected, *e.g.* threshold branch cuts, which on the lattice emerge as poles on the imaginary temporal axis, as depicted in Figure 4.

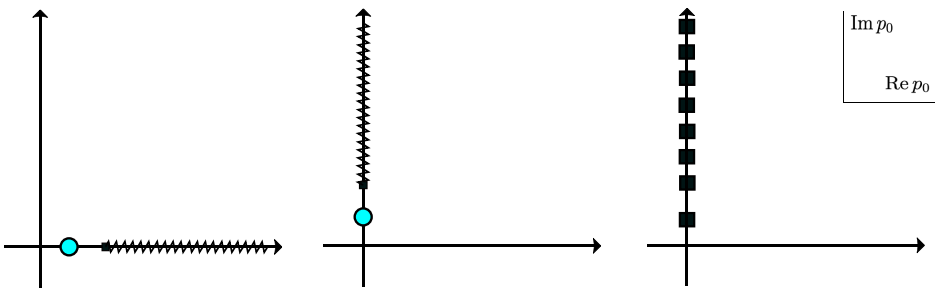

Figure 4: Scheme of amplitude's complex energy plane in the infinite volume (left), followed by Euclidean rotation (middle), and then compactification in space (right).

In the so-called Lüscher formalism, the finite-volume corrections to the spectrum in a periodic box are related to the two-particle scattering amplitude up to exponentially suppressed volume effects [5–7]. This was originally developed in the elastic regime for degenerate-mass particles overall at rest, and was later extended to general moving frames [8] and non-identical particles [25, 39]. This was also developed for a relativistic field theory [9], extended to multiple channels [40] and spinning particles [41].

The central object of the finite-volume formalism is the *quantisation condition*, which relates *power-like* finite-volume corrections on the spectrum to the elastic two-particle scattering amplitude, [9]

$$\det\left[1 + i\mathcal{M}\big(E_{\text{cm}}(L)\big)F\big(E_{\text{cm}}(L), L\big)\right] = 0\,, \tag{12}$$

where F is a known function and we made the L-dependence encoding the finite-volume corrections explicit. Note that both F and $\mathcal{M}$ depend on the CM energy E_{cm} and satisfy (12) precisely *at the finite-volume energies* $E_{\text{cm}}(L)$. Further note that Eq.(12) contains a determinant over angular momentum indices (ℓ, m), which can be block-diagonalised into lattice irreps Λ. In the case that only a single partial wave is relevant, that can be written as

$$\delta_1\big(E_{\text{cm}}(L)\big) = n\pi - \phi^{\Lambda}\big(E_{\text{cm}}(L), L, m_1, m_2\big), \quad n \in \mathbb{Z}, \tag{13}$$

where ϕ^{Λ} contains the angular components of F which project it into a definite lattice irrep Λ [17, 42]. It also depends on the rest-frame masses of the scattered particles, m_1 and m_2.

3.2 Pole Parameters

A resonance, say $K^*(892)$, can be viewed as an intermediate state of a scattering process such as $K\pi \to K^*(892) \to K\pi$. This is typically manifest as an enhancement of the total cross-section around the resonance rest mass. The width of a resonance is directly related to its *decay width*. In phenomenology, it is usual to parameterise the scattering phase shift through a Breit-Wigner-like distribution featuring a mass m_{BW}, a width Γ_{BW}, among other parameters [2].

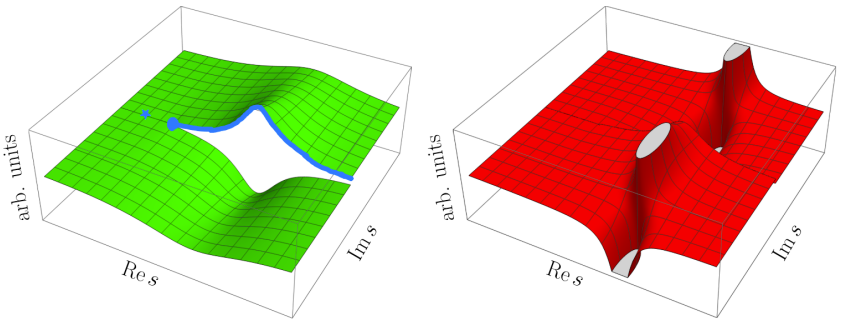

Figure 5: Imaginary parts of the multi-valued scattering amplitude. [2] The resonance poles appear on the second ("unphysical") sheet (red), affecting observables on the real-s line (blue) at the first ("physical") sheet.

A model-independent definition of resonances relates them to certain complex-energy *singularities* of partial-wave scattering amplitudes under analytical continuation. This description includes the pole position, written in terms of a mass M and width Γ as

$$\sqrt{s_R} = M - \frac{i}{2}\Gamma, \tag{14}$$

but also residues which are related to effective couplings [2]. From unitarity and causality constraints, resonance poles are required to appear on the second (or "unphysical") Riemann sheet of the amplitude t [43]. Figure 5 illustrates the singularities contained on an example amplitude and how they are analytically connected to the real axis behaviour, where scattering takes place.

4. Data Analysis

We now summarise the statistical analysis of the $K\pi$ and $\pi\pi$ scattering, taking into account the fit range systematic in the phase-shift and pole parameters determination. Because there is no

reference to the spacetime metric on $E_{\mathrm{cm}}(L)$ in the quantisation condition (13), the lattice energies $\{E_{\mathrm{cm}}\}$ computed from the GEVP eigenvalues can be used to extract the infinite-volume scattering phase shift at fixed L. For example, one could directly compute the phase shift *at* the discrete lattice energies. However, we aim to compute complex-energy poles from the amplitude, which can be achieved by constraining phase-shift *models* and analytically continuing them into the complex plane [14, 17].

Given a model δ_1^{mod} with parameters grouped into a vector $\boldsymbol{\alpha}^{\mathrm{mod}}$, we can invert Eq. (13) to obtain a set of finite-volume energies $\{\mathcal{E}_{\mathrm{cm}}(\boldsymbol{\alpha}^{\mathrm{mod}})\}$. The correlated difference between lattice energies and the ones predicted by the model leads to a chi-squared function whose minimisation leads to the constrained model parameters [44]. The resonance pole positions (14) can be found on the unphysical sheet of the model amplitudes, $t^{\mathrm{mod}}(\sqrt{s}) = \left(\cot\delta_1^{\mathrm{mod}}(\sqrt{s})|_{\boldsymbol{\alpha}^{\mathrm{mod}}} - i\right)^{-1}$, for complex $\sqrt{s}$. Depending on the model, this can be done either exactly or through a numerical procedure computing the resonance pole position within a certain small tolerance [18]. In this work, both the *Breit-Wigner* (BW) and the *effective range expansion* phase-shift models are employed.

We devise a procedure to estimate the systematics due to the variation of phase-shift model and GEVP eigenvalue fit ranges, inspired on recent calculations based on the *Akaike information criterion* (AIC) [45–48]

$$\mathrm{AIC} = \chi^2 + 2n^{\mathrm{par}} - n^{\mathrm{data}}\,, \tag{15}$$

where χ^2 is the chi-squared value resulting from a given fit, n^{par} is the number of model parameters and n^{data} the number of data points. The total systematic is based on the spread of the distribution of resonance parameters weighted by $w_{\mathrm{t}}(\mathsf{f},\mathsf{mod}) \propto \exp\left[-\frac{1}{2}\mathrm{AIC}_{\mathrm{t}}(\mathsf{f},\mathsf{mod})\right]$, where $\mathrm{AIC}_{\mathrm{t}}$ is the sum of the $\mathrm{AIC}_{\mathrm{corr}}$'s coming from all eigenvalue fits and the $\mathrm{AIC}_{\mathrm{PS}}$ from the phase-shift fit, given a collection of fit ranges $\{\mathsf{f}_{(1)},\mathsf{f}_{(2)},\ldots\} \equiv \mathsf{f}$. This distribution is not known a priori and the number of combinations f is too high for a brute-force computation. We instead resort to *importance sampling* with proposal distribution based on the $\mathrm{AIC}_{\mathrm{corr}}$ weights, which is at the end "reweighted" by the distribution based on the $\mathrm{AIC}_{\mathrm{PS}}$ weight [18]. We repeat this process varying the possible pool of fit ranges, thus providing an account of the uncertainty due to the importance sampling.

We take the 96% w_{PS}-weighted confidence interval over all samples as the "data-driven" systematic error. The statistical error is given by the bootstrap standard deviation of the w_{PS}-weighted mean. The final central values of the pole positions in lattice units are $(M_{K^*},\Gamma_{K^*}) \approx (893, 51)$ MeV, and $(M_\rho,\Gamma_\rho) \approx (796, 192)$ MeV. The data-driven systematic error amounts to $1-2\%$ for the mass and $15-20\%$ for the width, while the statistical errors are three to five times smaller than this systematic [18].

Is is a fact that the Lüscher formalism is strictly valid for finite-volume energies in the continuum. As this work only uses one lattice spacing and thus no continuum extrapolation, we further prescribe a systematic discretisation uncertainty of 5% based on naive power-counting arguments. Due to other unaccounted for effects, *e.g.* three-particle thresholds and quark-mass mismatch, we assume a total 6% "extra" systematic error. With the addition or not of this latter uncertainty, the final ρ and K^* pole positions are in reasonable agreement with the values derived directly from experimental data using effective theories and dispersion relations [2]. For full details and discussions, see Ref. [18, 19].

5. Conclusions

We computed resonance parameters of the $K^*(892)$ and $\rho(770)$ particles using first-principles lattice QCD simulations with a physical pion mass. We provided a thorough estimation of the systematic error inherent to the analysis of the lattice data. This involved the exploration of a model-averaging technique applied to the Lüscher method via the importance sampling of correlator fit ranges.

We implemented the distillation method within the `Grid` and `Hadrons` lattice code environment, which allowed for a large-scale calculation performed on two supercomputers from the STFC DiRAC Extreme Scaling service. Particularly expensive parts of the data were stored for further applications and the raw lattice observables were made publicly available [18]. The open-source nature of the code will allow for further improvements and applications [32, 33]. For instance, this code is being used as part of a calculation of hadronic D decays [49].

In view of the prescribed discretisation error, the most immediate improvement of this calculation would be the addition of more lattice spacings. Followed by a continuum extrapolation [50], this will allow for a even more direct comparison to experiment. Due to the high cost of the domain-wall action, this is particularly challenging and will rely on the advancement of dedicated lattice QCD software tailored to the next-generations of supercomputers.

Further use of the data or infrastructure developed in this work includes the study of the κ and σ scalar resonances [17, 51] and the radiative $K\gamma \to K\pi$ and $\pi\gamma \to \pi\pi$ transitions [52, 53]. Another possibility for future work is based on the recent interest towards Standard Model tests from experimental data in the search for new physics [54–57], which evidences the importance of a first-principles determination of weak decays such as $B \to K^*\ell^+\ell^-$ and $B \to \rho\ell\nu$ from lattice QCD [40, 58–60].

Acknowledgements

N.L. received funding from the European Research Council (ERC) under the European Union's Horizon 2020 research and innovation programme under grant agreement No 813942. This work used the DiRAC Extreme Scaling service at the University of Edinburgh, operated by the Edinburgh Parallel Computing Centre on behalf of the STFC DiRAC HPC Facility (`https://dirac.ac.uk/`). The equipment was funded by BEIS capital funding via STFC grants ST/R00238X/1 and STFC DiRAC Operations grant ST/R001006/1. DiRAC is part of the National e-Infrastructure. PB has been supported in part by the U.S. Department of Energy, Office of Science, Office of Nuclear Physics under the Contract No. DE-SC-0012704 (BNL). P.B. has also received support from the Royal Society Wolfson Research Merit award WM/60035. N.L. & A.P. received funding from the European Research Council (ERC) under the European Union's Horizon 2020 research and innovation programme under grant agreement No 813942. M.M. gratefully acknowledges support from the STFC in the form of a fully funded PhD studentship. A.P. & F.E. are supported in part by UK STFC grant ST/P000630/1. A.P. & F.E. also received funding from the European Research Council (ERC) under the European Union's Horizon 2020 research and innovation programme under grant agreements No 757646.

References

[1] R.A. Briceño, J.J. Dudek and R.D. Young, *Scattering processes and resonances from lattice QCD*, *Reviews of Modern Physics* **90** (2018) 25001 [1706.06223].

[2] R.L. Workman, V.D. Burkert, V. Crede, E. Klempt, U. Thoma, L. Tiator et al., *Review of Particle Physics (PDG)*, *Progress of Theoretical and Experimental Physics* **2022** (2022) 083C01.

[3] T. Aoyama et al., *The anomalous magnetic moment of the muon in the Standard Model*, *Phys. Rept.* **887** (2020) 1 [2006.04822].

[4] LHCb, *Test of Lepton Universality in $b \to s\ell^+\ell^-$ Decays*, *Physical Review Letters* **131** (2023) 51803.

[5] M. Lüscher, *Volume dependence of the energy spectrum in massive quantum field theories I*, *Communications in Mathematical Physics* **104** (1986) 177.

[6] M. Lüscher, *Volume dependence of the energy spectrum in massive quantum field theories II*, *Communications in Mathematical Physics* **105** (1986) 153.

[7] M. Lüscher, *Two-particle states on a torus and their relation to the scattering matrix*, *Nuclear Physics, Section B* **354** (1991) 531.

[8] K. Rummukainen and S. Gottlieb, *Resonance scattering phase shifts on a non-rest-frame lattice*, *Nuclear Physics B* **450** (1995) 397 [9503028].

[9] C.H. Kim, C.T. Sachrajda and S.R. Sharpe, *Finite-volume effects for two-hadron states in moving frames*, *Nuclear Physics B* **727** (2005) 218 [0507006].

[10] M.T. Hansen, *Pushing the Periodic Boundaries*, *Proceedings of The 38th International Symposium on Lattice Field Theory — PoS(LATTICE2021)* **396** (2022) 024.

[11] M. Peardon, J. Bulava, J. Foley, C.J. Morningstar, J.J. Dudek, R.G. Edwards et al., *Novel quark-field creation operator construction for hadronic physics in lattice QCD*, *Physical Review D* **80** (2009) 054506.

[12] M. Lüscher, *Computational Strategies in Lattice QCD*, *Lectures given at the Summer School on "Modern perspectives in lattice QCD", Les Houches* (2010) [1002.4232].

[13] A.D. Hanlon, *Hadron spectroscopy and few-body dynamics from lattice QCD*, *Proceedings of The 40th Annual International Symposium on Lattice Field Theory — PoS(LATTICE2023)* (2024) [2402.05185].

[14] D.J. Wilson, R.A. Briceño, J.J. Dudek, R.G. Edwards and C.E. Thomas, *Coupled $\pi\pi, K\bar{K}$ scatterin gin P-wave and the ρ resonance from lattice QCD*, *Physical Review D* **92** (2015) 094502 [arXiv:1507.02599v2].

[15] F.B. Erben, J.R. Green, D. Mohler and H. Wittig, *Rho resonance, timelike pion form factor, and implications for lattice studies of the hadronic vacuum polarization*, *Physical Review D* **101** (2020) 054504 [1910.01083].

[16] D.J. Wilson, R.A. Briceño, J.J. Dudek, R.G. Edwards and C.E. Thomas, *Quark-Mass Dependence of Elastic πk Scattering from QCD*, *Physical Review Letters* **123** (2019) 1 [arXiv:1904.03188v1].

[17] G. Rendon, L. Leskovec, S. Meinel, J. Negele, S. Paul, M. Petschlies et al., *I = 1/2 S-wave and P-wave Kπ scattering and the κ and K* resonances from lattice QCD*, *Physical Review D* **102** (2020) 114520 [2006.14035].

[18] P.A. Boyle, F. Erben, V. Gülpers, M.T. Hansen, F. Joswig, N. Pitanga Lachini et al., *Physical-mass calculation of ρ(770) and K*(892) resonance parameters via ππ and Kπ scattering amplitudes from lattice QCD*, 2406.19193.

[19] P.A. Boyle, F. Erben, V. Gülpers, M.T. Hansen, F. Joswig, N. Pitanga Lachini et al., *Light and strange vector resonances from lattice QCD at physical quark masses*, 2406.19194.

[20] N.P. Lachini, P.A. Boyle, F.B. Erben, M. Marshall and A. Portelli, *Kπ scattering at physical pion mass using distillation*, *Proceedings of Science* **396** (2022) 1 [2112.09804].

[21] N.P. Lachini, P.A. Boyle, F.B. Erben, M. Marshall and A. Portelli, *Towards Kπ scattering with domain-wall fermions at the physical point using distillation*, in *Proceedings of The 39th International Symposium on Lattice Field Theory — PoS(LATTICE2022)*, (Trieste, Italy), p. 076, Sissa Medialab, mar, 2023, DOI [arXiv:2211.16601v1].

[22] T. Blum, P.A. Boyle, N.H. Christ, J. Frison, N. Garron, R.J. Hudspith et al., *Domain wall QCD with physical quark masses*, *Physical Review D* **93** (2016) 074505 [1411.7017].

[23] C.E. Thomas, R.G. Edwards and J.J. Dudek, *Helicity operators for mesons in flight on the lattice*, *Physical Review D* **85** (2012) 014507 [1107.1930].

[24] J. Elliot and P.G.Dawber, *Symmetry in Physics. Vol. 1: Principles and Simple Applications* (1987).

[25] L. Leskovec and S. Prelovsek, *Scattering phase shifts for two particles of different mass and nonzero total momentum in lattice QCD*, *Physical Review D* **85** (2012) 114507 [arXiv:1202.2145].

[26] J.E. Mandula, G. Zweig and J. Govaerts, *Representations of the Rotation Reflection Symmetry Group of the Four-dimensional Cubic Lattice*, *Nucl. Phys. B* **228** (1983) 91.

[27] D.C. Moore and G.T. Fleming, *Angular momentum on the lattice: The Case of non-zero linear momentum*, *Phys. Rev. D* **73** (2006) 014504 [hep-lat/0507018].

[28] C. Morningstar, J. Bulava, J. Foley, K.J. Juge, D. Lenkner, M. Peardon et al., *Improved stochastic estimation of quark propagation with Laplacian Heaviside smearing in lattice QCD*, *Physical Review D* **83** (2011) 114505 [1104.3870].

[29] C.J. Morningstar and M. Peardon, *Analytic smearing of SU(3) link variables in lattice QCD*, *Physical Review D* **69** (2004) 054501 [0311018].

[30] A. Portelli, *Hadrons: a Grid-powered workflow management system for lattice QCD measurements*, in *37th International Symposium on Lattice Field Theory (LATTICE2019)*, 2019, https://indi.to/9RQpb.

[31] N.P. Lachini and F.B. Erben, *Distillation documentation - Hadrons*, *https://aportelli.github.io/Hadrons-doc/#/mdistil* (2022) .

[32] A. Portelli, R. Abott, N. Asmussen, A. Barone, P.A. Boyle, F.B. Erben et al., *aportelli/Hadrons: Hadrons v1.4*, *10.5281/zenodo.8023716* (2023) .

[33] P.A. Boyle, A. Yamaguchi and A. Portelli, *Grid: A next generation data parallel C++ QCD library*, in *The 33rd International Symposium on Lattice Field Theory*, Sissa, 2015.

[34] M. Lüscher and U. Wolff, *How to calculate the elastic scattering matrix in two-dimensional quantum field theories by numerical simulation*, *Nuclear Physics, Section B* **339** (1990) 222.

[35] B. Blossier, M.D. Morte, G.V. Hippel, T. Mendes and R. Sommer, *On the generalized eigenvalue method for energies and matrix elements in lattice field theory*, *Journal of High Energy Physics* **2009** (2009) [0902.1265].

[36] M.E. Peskin and D.V. Schroeder, *An Introduction to Quantum Field Theory*, Frontier of Physics, Westview Press, Boulder (1995).

[37] L. Maiani and M. Testa, *Final state interactions from euclidean correlation functions*, *Physics Letters B* **245** (1990) 585.

[38] H.B. Meyer, *Photodisintegration of a Bound State on the Torus*, 1202.6675.

[39] Z. Fu, *Rummukainen-Gottlieb formula on a two-particle system with different masses*, *Physical Review D* **85** (2012) 014506 [1110.0319].

[40] M.T. Hansen and S.R. Sharpe, *Multiple-channel generalization of Lellouch-Lüscher formula*, *Physical Review D* **86** (2012) 016007 [1204.0826].

[41] R.A. Briceño, *Two-particle multichannel systems in a finite volume with arbitrary spin*, *Physical Review D - Particles, Fields, Gravitation and Cosmology* **89** (2014) 1 [1401.3312].

[42] A. Alexandru, L. Leskovec, S. Meinel, J. Negele, S. Paul, M. Petschlies et al., *P -wave ππ scattering and the ρ resonance from lattice QCD*, *Physical Review D* **96** (2017) 1 [arXiv:1704.05439v2].

[43] V. Gribov, *Strong Interactions of Hadrons at High Energies*, Cambridge University Press, Cambridge (2008), 10.1017/CBO9780511534942.

[44] P. Guo, J.J. Dudek, R.G. Edwards and A.P. Szczepaniak, *Coupled-channel scattering on a torus*, *Physical Review D - Particles, Fields, Gravitation and Cosmology* **88** (2013) 1 [1211.0929].

[45] H. Akaike, *A new look at the statistical model identification*, *IEEE Transactions on Automatic Control* **19** (1974) 716.

[46] S. Borsanyi, S. Durr, Z. Fodor, C. Hoelbling, S.D. Katz, S. Krieg et al., *Ab initio calculation of the neutron-proton mass difference*, *Science* **347** (2015) 1452 [1406.4088].

[47] S. Borsanyi, Z. Fodor, J.N. Guenther, C. Hoelbling, S.D. Katz, L. Lellouch et al., *Leading hadronic contribution to the muon magnetic moment from lattice QCD*, *Nature* **593** (2021) 51 [2002.12347].

[48] W.I. Jay and E.T. Neil, *Bayesian model averaging for analysis of lattice field theory results*, *Physical Review D* **103** (2021) 114502 [2008.01069].

[49] F.B. Erben, M.T. Hansen, F. Joswig, N.P. Lachini and A. Portelli, *Exploring distillation at the SU(3) flavour symmetric point*, *LATTICE2022, 39th International Symposium on Lattice Field Theory* (2022) [arXiv:2211.15627].

[50] M.T. Hansen and T. Peterken, *Discretization effects in finite-volume* $2 \to 2$ *scattering*, 2408.07062.

[51] R.A. Briceño, J.J. Dudek, R.G. Edwards and D.J. Wilson, *Isoscalar $\pi\pi$ Scattering and the σ Meson Resonance from QCD*, *Physical Review Letters* **118** (2017) .

[52] C. Alexandrou, L. Leskovec, S. Meinel, J. Negele, S. Paul, M. Petschlies et al., *$\pi\gamma \to \pi\pi$ transition and the ρ radiative decay width from lattice QCD*, *Physical Review D* **98** (2018) 1 [arXiv:1807.08357v5].

[53] A. Radhakrishnan, J.J. Dudek and R.G. Edwards, *Radiative decay of the resonant K^* and the $\gamma K \to K\pi$ amplitude from lattice QCD*, *Physical Review D* **106** (2022) 114513 [arXiv:2208.13755v1].

[54] F.U. Bernlochner, Z. Ligeti and S. Turczyk, *New ways to search for right-handed current in $B \to \rho\ell\bar{\nu}$*, *Physical Review D* **90** (2014) 094003 [1408.2516].

[55] M. Algueró, B. Capdevila, A. Crivellin, S. Descotes-Genon, P. Masjuan, J. Matias et al., *Emerging patterns of New Physics with and without Lepton Flavour Universal contributions*, *European Physical Journal C* **79** (2019) 1 [1903.09578].

[56] R. Aaij, A.S. Abdelmotteleb, C. Abellan Beteta, F. Abudinén, T. Ackernley, B. Adeva et al., *Test of Lepton Universality in $b \to s\ell^+\ell^-$ Decays*, *Physical Review Letters* **131** (2023) 51803 [2212.09152].

[57] Belle II Collaboration, F. Abudinén, I. Adachi, K. Adamczyk, L. Aggarwal, P. Ahlburg et al., *Reconstruction of $B \to \rho\ell\nu_\ell$ decays identified using hadronic decays of the recoil B meson in 2019 – 2021 Belle II data*, *arXiv* (2022) 1 [2211.15270].

[58] L. Lellouch and M. Lüscher, *Weak transition matrix elements from finite-volume correlation functions*, *Communications in Mathematical Physics* **219** (2001) 31.

[59] A. Agadjanov, V. Bernard, U.G. Meißner and A. Rusetsky, *The $B \to K^*$ form factors on the lattice*, *Nuclear Physics B* **910** (2016) 387.

[60] L. Leskovec, S. Meinel, M. Petschlies, J. Negele and S. Paul, *A lattice QCD study of the $B \to \pi\pi\ell\nu$*, *The 39th International Symposium on Lattice Field Theory - PoS(LATTICE2022)* (2022) [arXiv:2212.08833v2].